



Koninklijk Nederlands
Meteorologisch Instituut
Ministerie van Infrastructuur en Milieu



CHEFS

C-band High and Extreme-force Speeds

EUMETSAT ITT 16/166

WP2: State of the art and user requirements

KNMI, de Bilt
The Netherlands

supported by ICM, Spain, and IFREMER, France

2 October 2018

DOI: 10.13140/RG.2.2.10541.13281

Cover photograph:

Sea state in hurricane Ike (2009) for recorded SFMR winds of 85 knots (43 m/s; 157 km/hr) and flight level winds (at 2.4 km) of 125 knots (64 m/s; 232 km/hr). Large white foam patches, wave fronts, but no apparent sea state saturation (nor uniformity).

© Ad Stoffelen

Submitted to:

The European Organisation for the Exploitation of Meteorological Satellites (EUMETSAT)

Prime author:

Ad Stoffelen, KNMI

Tel: +31 6 2240 9813

R&D Satellite Observations

Head Active Sensing group

E-mail: Ad.Stoffelen@KNMI.NL

Postbus 201

3730 AE de Bilt

The Netherlands

With acknowledged contributions from:

Marcos Portabella, ICM, Barcelona, Spain

Alexis Mouche, IFREMER, Brest, France

Gerd-Jan van Zadelhoff, KNMI, the Netherlands

Federica Polverari, ICM, Barcelona, Spain

Wenming Lin, NUIST, Nanjing, China

Joseph Sapp, NOAA, College Park MD, USA

Paul Chang, NOAA, College Park MD, USA

Zorana Jenenak, College Park MD, USA

Jean-Raymond Bidlot, ECMWF, Reading, UK

Mark Bourassa, FSU, Tallahassee FL, USA

Doug Vandemark, UNH, Durham NH, USA

James Edson, University of Connecticut, Storrs, USA

Lucia Pineau-Guillou, IFREMER, Issy-les-Moulineaux, France

Stefanie Linow, EUMETSAT, Germany

TABLE OF CONTENTS

1.	INTRODUCTION	5
1.1.	EXTREME WINDS IN METEOROLOGICAL SERVICES	5
1.2.	SCATTEROMETRY	6
1.3.	REFERENCES	7
1.4.	ACRONYMS	11
2.	STATE OF THE ART IN OCEAN WIND SENSING	14
2.1.	C-BAND RADAR	14
2.2.	SCA INSTRUMENT	14
2.3.	SAR REFERENCE DATA	15
2.4.	OTHER SATELLITE SENSORS	15
3.	WIND REFERENCES	17
3.1.	WIND CALIBRATION REFERENCES FOR HIGH AND EXTREME OSVW	17
3.2.	NOAA HURRICANE HUNTERS	18
3.3.	OTHER HIGH-WIND SOURCES	19
3.4.	COMPARING EXTREME WIND DATA	19
3.5.	THE INCONSISTENCY OF HIGH AND EXTREME WIND REFERENCES	20
3.6.	USER REQUIREMENTS	21
4.	THE NEXT STEPS FOR OBTAINING CALIBRATED EXTREME SATELLITE WINDS	22
4.1.	APPROACH FOR MOORED BUOY REFERENCE	22
4.2.	APPROACH FOR DROPSONDES	23
4.3.	NWP REFERENCE	24
4.4.	SAR DATA ASSESSMENT	24
4.5.	SATELLITE WIND REFERENCE	25
5.	EXECUTIVE SUMMARY	26

FIGURES

Figure 2.1: An example of measured ASCAT scatterometer hurricane winds, explained at projects.knmi.nl/scatterometer/tile_prod/tile_app.cgi. Winds up to 70 knots or 35 m/s are measured by ASCAT in speed-coloured flags for this case, while the collocated ECMWF winds are plotted in green. 16

Figure 3.1. Illustration of modified (2012) SFMR wind speeds (blue), rain rate, RR, (red) and collocated ASCAT speed, V, (green) and SFMR-ASCAT speed difference. SFMR speeds have been ad hoc modified to match ASCAT over a large number of typhoons. This matching required subtraction of $\ln(RR)$ and $\ln(V)$ and provides an estimate of current typical calibration uncertainty. Although uncertain, the ASCAT depiction of typhoon structure appears generally faithful up to 35 m/s. 17

Figure 3.2: ASCAT acquisitions of maximum wind early October 2014 up to 42 m/s (150 km/h). ASCAT-A appears low as compared to ASCAT-B due to the 2014 calibration bias of ASCAT-B minus ASCAT-A of ~ 0.1 dB, where required accuracy is 0.2 dB (which nominally corresponds to ~ 0.2 m/s). Due to VV GMF saturation, 0.1 dB at 40 m/s is about 4 m/s. For extremes additional capability and/or more careful instrument calibration is needed [30]. 18

Figure 3.3: Simulated wind speed and direction difference statistics of X minus Y as a function of average wind speed, $(X+Y)/2$, for a global true wind speed distribution. Speed bias (thin solid line), standard deviation (thick solid line), direction bias (thin dotted line), standard deviation (thick dotted line), and vector root-mean-square (dashed line) of differences are shown. The simulation is done with the scatterometer wind distribution as "truth" and wind component standard errors of 1.0 and 1.8 ms^{-1} for X and Y, respectively. © [3]20

Figure 3.4: ASCAT wind speed scatter plots of a) ASCAT versus drop sondes (from [37]), b) ASCAT versus moored buoy winds and c) ECMWF NWP winds versus ASCAT. Using drop sondes, moored buoy winds and NWP references above 15 m/s may result in discrepancies due to height and position representation differences. 21

Figure 4.1: Archived buoy winds collected from NDBC, TAO, PIRATA and RAMA versus the same winds received in NRT over the WMO GTS (left) over 2009-2014. The scatter-density plot features colors on the scale, <1%, <10%, <20% ... <90% of the maximum bin value. Archive-GTS speed bias versus GTS-reported speed (right), which appears negligible. (courtesy, Wenming Lin, NUIST) 23

Figure 4.2: Wind speed PDF of archived buoy winds collected from NDBC, TAO, PIRATA and RAMA (Cwind), as collocated with the same data received by GTS at ECMWF (called MARS; purple), vice versa (red), Cwind PDF if no GTS found (blue) and vice versa (black). Red and purple are plotted in Figure 4.1. versus the same winds received in NRT over the WMO GTS (left). Archive-GTS speed bias versus GTS-reported speed (right), which appears negligible. Red and purple correspond to 3.2 million collocations, black to 3.3 million points and blue to 1.7 million. Collocation is successful when location, hour and heights match. (courtesy, Wenming Lin, NUIST) 23

1. Introduction

The first work package in CHEFS is to define the problem, objectives and activities in the project. After a brief introduction on the meteorological services that benefit from extreme satellite ocean surface vector winds and on the topic of scatterometry, we describe the state of the art in ocean wind sensing, the use of C-band radar and other satellite sensors. Section three addresses available wind references for satellite wind product calibration and section four addresses their use in CHEFS to obtain consolidated satellite wind products.

1.1. Extreme winds in meteorological services

The atmosphere is dynamic on scales from minutes to years. Processes involve among others turbulence, convection, wind, transport, mixing and gravity waves. Such processes affect economy and society. Moreover, the weather is transient and moves fast from one location to the next, thereby implying the need for international exchange of weather information. As such, it is not surprising that the World Meteorological Organization (WMO) [22] was established soon after the initiation of the first national meteorological offices about 150 years ago. Given the importance of meteorology for many aspects of life on Earth, under WMO auspices systematic conventional observations of the atmosphere have been acquired over the last centuries by national agencies, while recently also atmospheric satellite observations were introduced to further monitor and explore the Earth's atmosphere. Also these satellite observations are coordinated by WMO and the Committee on Earth Observation Satellites (CEOS)[24].

Several integrated meteorological applications are relevant for economy and society:

- Nowcasting;
- Short-range NWP;
- Medium-range NWP;
- Seasonal forecasting;
- Climate monitoring.

Meteorological services are generally well established and accessible through user requirement assessments, internationally coordinated space and ground-based observation networks and public national meteorological services or satellite agencies, which provide the core meteorological infrastructure. Private weather enterprises offer further downstream services. OSVW and wind stress force the ocean in many ways, where most uncertainty exists in these interaction processes at mesoscales and at extreme winds.

High and extreme winds play a disproportionately large role in Earth's weather and climate. Mid and high latitude high-wind events (cold air outbreaks) lasting several days, can remove what at typical wind speeds would be a month's worth of the ocean's heat and moisture, leading to the formation of "deep water" that helps drive global ocean circulation patterns. High winds also help exchange disproportionately large amounts of carbon dioxide. Moreover, long-term stable instrument records are essential to build confidence in the fidelity and limitations of model reanalyses and guide their application [40,41] in , e.g., civil protection and wind energy applications [55].

Global information on the motion near the ocean surface is generally lacking, limiting the physical modelling capabilities of the forcing of the world's water surfaces by the atmosphere. This also limits our knowledge of the exchange of momentum across the water-air interface, affecting meteorological and ocean applications. This knowledge is particularly important in extreme conditions of winds, waves and surges, which occur in tropical areas due to convective systems, in polar lows and in tropical and extratropical storms and hurricanes.

In nowcasting, for example, the Saffir-Simpson scale for tropical hurricane categories is crucial and central in the warning advisories of the National Hurricane Centre (NHC) in Miami, USA. This scale is based on the maximum 1-minute sustained 10m winds in the hurricane, but how can we know this?

“Maximum” implies a spatial survey of the hurricane wind conditions at 10 meter height, but is rather hard to obtain, as is discussed later. Satellite measurements in fact could provide wind maps of the hurricane over water, when they incidentally pass over the hurricane. Not surprisingly, this spatial information, from instruments such as the ASCAT scatterometer, proves to be very valuable in storm and hurricane conditions [56]. However, forecasters will need to use guidance to interpret the 20-km scale ASCAT 10m winds in terms of 1-minute sustained winds [57].

In NWP, spatial grids used for analysis and forecasting become finer in due time and in consequence the spatial resolution of NWP fields in extreme events allows in principle a better depiction of these events. The magnitude of extreme winds in NWP fields, however, depends on parameterisations of the ocean drag. To develop these parameterisations, a calibrated wind reference for such extreme conditions is paramount. This requirement becomes more pressing as the resolution of NWP models increases.

1.2. Scatterometry

A wind scatterometer provides 10m-height stress-equivalent winds on a scale of 12.5 or 25 km over the ocean surface and information on horizontal wind variability for, inter alia, weather warnings, climate monitoring and research on processes, ocean forcing and air-sea interaction or wind resource mapping. Moreover, a wind scatterometer, particularly at C band, has the capability to provide all-weather measurements, including in extreme conditions, e.g., in tropical convective systems and hurricanes, which are particularly relevant for the safety during off-shore activities and where other measurement techniques fail to provide adequate responses over large areas. I.e., in cases corresponding with extreme winds, waves and tides, where in situ measurements may be hazardous and unreliable. However, this also poses a challenge to develop and verify wind scatterometer processing algorithms for high and extreme winds.

In order to provide the EUMETSAT users with relevant atmospheric weather and climate conditions, KNMI, ICM and IFREMER carry out the CHEFS study, which is based on operational experience by the partners, gained over the last decades.

Through this report, KNMI starts the study with establishing a brief overview of the state of the art in C-band scatterometer high and extreme wind speed retrievals, based on the experience of the project team and their several publications on the topic. This overview includes current and prospective user requirements from the various application areas (nowcasting, NWP, oceanography, climate) and a related description of (partial) compliance of current and future C-band scatterometer missions and a comparison with surface wind references and surface wind speed missions, as expected in the EPS SG era.

The extension of the current ASCAT operational wind services to more reliable extreme winds with SCA, using the various polarization options, will be elaborated and summarized. The project team will also document the possibility of using Doppler information at extreme winds, following further SAG discussions on SCA Doppler capability.

1.3. References

- [1] Anderson, C., J. Figa, H. Bonekamp, J. Wilson, J. Verspeek, A. Stoffelen and M. Portabella, *Validation of Backscatter Measurements from the Advanced Scatterometer on MetOp-A*, J. Atm. Oceanic Technol., 2012, **29**, 77-88.
- [2] Vogelzang, J., A. Stoffelen, A. Verhoef and J. Figa-Saldana, *On the quality of high-resolution scatterometer winds*, J. Geophys. Res., 2011, **116**, C10033, [doi:10.1029/2010JC006640](https://doi.org/10.1029/2010JC006640).
- [3] Stoffelen, Ad *Toward the true near-surface wind speed: Error modeling and calibration using triple collocation*, J. GEOPH. RES **103** (C4), 7755-7766, 1998, [doi:10.1029/97JC03180](https://doi.org/10.1029/97JC03180).
- [5] Portabella, M., A. Stoffelen, W. Lin, A. Turiel, A. Verhoef, J. Verspeek and J. Ballabrera-Poy, *Rain Effects on ASCAT-Retrieved Winds: Toward an Improved Quality Control*, IEEE Transactions on Geoscience and Remote Sensing, PP, 2012, **99**, 1-12, [doi:10.1109/TGRS.2012.2185933](https://doi.org/10.1109/TGRS.2012.2185933).
- [6] Portabella, M., A. Stoffelen, A. Verhoef and J. Verspeek, *A new method for improving ASCAT wind quality control*, IEEE Gosci. Remote Sensing Letters, 2012, **9**, 4, 579-583, [doi:10.1109/LGRS.2011.2175435](https://doi.org/10.1109/LGRS.2011.2175435).
- [7] Verhoef, A., M. Portabella and A. Stoffelen, *High-resolution ASCAT scatterometer winds near the coast*, IEEE Transactions on Geoscience and Remote Sensing, 2012, **50**, 7, 2481-2487, [doi:10.1109/TGRS.2011.2175001](https://doi.org/10.1109/TGRS.2011.2175001).
- [9] Vogelzang, J. and A. Stoffelen, *NWP Model Error Structure Functions obtained from Scatterometer Winds*, IEEE Transactions on Geoscience and Remote Sensing, 2012, **50**, 7, 2525-2533, [doi:10.1109/TGRS.2011.2168407](https://doi.org/10.1109/TGRS.2011.2168407).
- [10] Vogelzang, J. and A. Stoffelen, *Scatterometer wind vector products for application in meteorology and oceanography*, Journal of Sea Research, 74, 2012, 74, 74, 16-25, [doi:10.1016/j.seares.2012.05.002](https://doi.org/10.1016/j.seares.2012.05.002).
- [13] Vandemark, Doug, James Edson and Marc Emond, 2018, [Evaluating several key issues in satellite wind stress validation](https://www.mdc.coaps.fsu.edu/scatterometry/meeting/docs/2018/docs/WednesdayApril25/WednesdayMorning/vandemark_edson_OVW2018_talk.pptx), IOVWST meeting, Barcelona Spain, April 24-26, 2018, [mdc.coaps.fsu.edu/scatterometry/meeting/docs/2018/docs/WednesdayApril25/WednesdayMorning/vandemark_edson_OVW2018_talk.pptx](https://www.mdc.coaps.fsu.edu/scatterometry/meeting/docs/2018/docs/WednesdayApril25/WednesdayMorning/vandemark_edson_OVW2018_talk.pptx)
- [14] Verspeek, J.A., A. Stoffelen, M. Portabella, H. Bonekamp, C. Anderson and J. Figa, *Validation and calibration of ASCAT using CMOD5.n*, IEEE Transactions on Geoscience and Remote Sensing, 2010, **48**, 1, 386-395, [doi:10.1109/TGRS.2009.2027896](https://doi.org/10.1109/TGRS.2009.2027896).
- [15] Portabella, M. and A.C.M. Stoffelen, *On Scatterometer Ocean Stress*, J. Atm. Oceanic Technol., 2009, **26**, 2, 368-382, [doi:10.1175/2008JTECHO578.1](https://doi.org/10.1175/2008JTECHO578.1).
- [16] Vogelzang, J., A. Stoffelen, A. Verhoef, J. de Vries and H. Bonekamp, *Validation of two-dimensional variational ambiguity removal on SeaWinds scatterometer data*, J. Atm. Oceanic Technol., 7, 2009, 26, 1229-1245, [doi:10.1175/2008JTECHA1232.1](https://doi.org/10.1175/2008JTECHA1232.1).
- [17] Portabella, M. and A. Stoffelen, *Scatterometer backscatter uncertainty due to wind variability*, IEEE Transactions on Geoscience and Remote Sensing, 2006, **44**, 11, 3356-3362, [doi:10.1109/TGRS.2006.877952](https://doi.org/10.1109/TGRS.2006.877952), available from www.knmi.nl/scatterometer/publications.
- [18] Stoffelen, A. and M. Portabella, *On Bayesian Scatterometer Wind Inversion*, IEEE Transactions on Geoscience and Remote Sensing, 2006, **44**, 6, 1523-1533, [doi:10.1109/TGRS.2005.862502](https://doi.org/10.1109/TGRS.2005.862502), available from www.knmi.nl/scatterometer/publications.
- [19] Portabella, M. and A. Stoffelen, *A probabilistic approach for SeaWinds data assimilation*, Quart. J. Royal Meteor. Soc., 2004, **130**, 596, 127-159, [doi:10.1256/qj.02.205](https://doi.org/10.1256/qj.02.205), available from www.knmi.nl/scatterometer/publications
- [20] Hersbach, H., A. Stoffelen and S. de Haan, *An Improved C-band scatterometer ocean geophysical model function: CMOD5*, J. Geophys. Res., 2007, **112**, C03006, [doi:10.1029/2006JC003743](https://doi.org/10.1029/2006JC003743).

- [21] Position Paper – Post-EPS Developments on Atmospheric Sounding and Wind Profiling, Ad Stoffelen, Massimo Bonavita, John Eyre, Mitchell Goldberg, Heikki Järvinen, Carmine Serio, Jean-Noël Thépaut, Volker Wulfmeyer, EUMETSAT, 10/11/2006;
- Cloud, Precipitation and Large Scale Land Surface Imaging (CPL) Observational Requirements for Meteorology, Hydrology and Climate, R. Rizzi, P. Bauer, S. Crewell, M. Leroy, C. Mätzler, W. P. Menzel, B. Ritter, J.E. Russell, A. Thoss;
- Post-EPS: Generic Requirements on Climate Monitoring, Simon Tett, John Bates, Reinout Boers, Alain Chédin, Steven Dewitte, Mark McCarthy, Jörg Schulz, Werner Thomas;
- Requirements for Operational Atmospheric Chemistry Monitoring in the Post-EPS Time Frame beyond 2020, H. Kelder, B. Kerridge, I. Isaksen, B. Carli, N. Harris, E. Hilsenrath
- www.eumetsat.int/Home/Main/Satellites/PostEPS/Resources/index.htm?l=en .
- [22] WMO :
- Gap analysis and Rolling Requirements Review,
www.wmo.int/pages/prog/sat/Databases.html#UserRequirements
- Nowcasting, www.wmo.int/pages/prog/amp/pwsp/Nowcasting.htm
- NWP, wmo-workshop-on-the-use-of-nwp-for-nowcasting.wikispaces.com/
- Wind farms: www.wmo.int/pages/prog/www/IMOP/reports/2009/Final%20Report%20ET-SBRSo%20and%20ET-RSUTT.pdf
- [23] Stoffelen, Ad, Jean Pailleux, Erland Källén, J. Michael Vaughan, Lars Isaksen, Pierre Flamant, Werner Wergen, Erik Andersson, Harald Schyberg, Alain Culoma, Roland Meynard, Martin Endemann, and Paul Ingmann, The Atmospheric Dynamics Mission for global wind field measurement, BAMS, Jan 2005, 73-87.
- ADM-Aeolus Science Report, ESA SP-1311;
esamultimedia.esa.int/docs/SP-1311_ADM-Aeolus_FINAL_low-res.pdf
- www.esa.int/esaLP/ESAFZ92VMOC_LPAdmaeolus_0.html
- [24] CEOS – Committee on Earth Observation Satellites:
Earth Observation Handbook, www.eohandbook.com/eohb05/ceos/part3_3.html
- Virtual Constellation on Ocean Surface Vector Winds,
www.ceos.org/index.php?option=com_content&view=category&layout=blog&id=73&Itemid=72
- [25] Scatterometer winds:
- [EUMETSAT Ocean and Sea Ice Satellite Application Facility](#)
 - [EU GMES MyOcean Monitoring and Forecasting](#)
 - [EU GMES MyWave Wave Monitoring and Forecasting](#)
 - [eSurge Satellite information for Storm Surges](#)
 - [EU Atlas for Wind Energy at Sea](#)
 - [3rd wind/wave forecasters training in May 2012, Brazil:](#) also
<http://cursos.cptec.inpe.br/marine-training-workshop/>
 - [Video 2nd wind/wave forecasters training in December 2011, Oostende](#)
- [26] ARGOSS BMT wave climate, www.waveclimate.com
- [27] Hurricane Forecast Improvement Program (HFIP),
NOAA, www.hfip.org/documents/hfip_pubs_2012.pdf
- [28] ESA Living Planet Programme,
http://www.esa.int/Our_Activities/Observing_the_Earth/The_Living_Planet_Programme

- [29] Brink, H.W. van den en G.P. Konnen, *Estimating 10000-year return values from short time series*, Int. J. Climatology, 2011, **31**, 115-126, [doi:10.1002/joc.2047](https://doi.org/10.1002/joc.2047).
- Haarsma, R.J., W. Hazeleger, C. Severijns, H. de Vries, A. Sterl, R. Bintanja, G.J. van Oldenborgh en H.W. van den Brink, *More hurricanes to hit Western Europe due to global warming*, Geophys. Res. Lett., 2013, [doi:10.1002/grl.50360](https://doi.org/10.1002/grl.50360).
- Brink, H.W. van den, G.P. Können, J.D. Opsteegh, G.J. van Oldenborgh en G. Burgers, *Estimating return periods of extreme events from ECMWF seasonal forecast ensembles*, Int. J. Climatology, 2005, **25**, 1345-1354, [doi:10.1002/joc.1155](https://doi.org/10.1002/joc.1155).
- [30] Belmonte Rivas, M., A. Stoffelen, J. Verspeek, A. Verhoef, X. Neyt and C. Anderson, *Cone metrics: a new tool for the intercomparison of scatterometer records*, accepted, IEEE Journal of Selected Topics in Applied Earth O, 2017, dx.doi.org/10.1109/JSTARS.2017.2647842.
- [31] Zadelhoff, G.J. van, A. Stoffelen, P.W. Vachon, J. Wolfe, J. Horstmann and M. Belmonte-Rivas, *Retrieving hurricane wind speeds using cross-polarization C-band measurements*, Atmospheric Measurement Techniques, 2014, **7**, 473-449, [doi:10.5194/amt-7-437-2014](https://doi.org/10.5194/amt-7-437-2014).
- [32] Belmonte-Rivas, M., A. Stoffelen and G.J. van Zadelhoff, *The Benefit of HH and VH Polarizations in Retrieving Extreme Wind Speeds for an ASCAT-Type Scatterometer*, IEEE Geosci. Remote Sensing Letters, 2014, **52**, 7, 4273-4280, [doi:10.1109/TGRS.2013.2280876](https://doi.org/10.1109/TGRS.2013.2280876).
- [33] Lin, C.C., M. Betto, M. Belmonte-Rivas, A. Stoffelen and J. de Kloe, *EPS-SG Wind scatterometer Concept Trade-offs and Wind Retrieval Performance Assessment*, IEEE Transactions on Geoscience and Remote Sensing, 2012, **50**, 7, 2458-2472, [doi:10.1109/TGRS.2011.2180393](https://doi.org/10.1109/TGRS.2011.2180393).
- [34] Mouche A., Chapron B., *Global C-Band Envisat, RADARSAT-2 and Sentinel-1 SAR measurements in copolarization and cross-polarization*. J. of Geophys. Research-oceans, 120(11), 7195- 7207, 2015. <http://doi.org/10.1002/2015JC011149> , OpenAccess version : archimer.ifremer.fr/doc/00289/40022.
- [35] J. W. Sapp, S. O. Alsheiss, Z. Jelenak, P. S. Chang, S. J. Frasier and J. Carswell, *Airborne Co-polarization and Cross-Polarization Observations of the Ocean-Surface NRCS at C-Band*, in IEEE Transactions on Geoscience and Remote Sensing, vol. 54, no. 10, pp. 5975-5992, Oct. 2016. [doi: 10.1109/TGRS.2016.2578048](https://doi.org/10.1109/TGRS.2016.2578048).
- Joe Sapp, Suleiman Alsheiss, Zorana Jelenak, Paul Chang, Steve Frasier*, Tom Hartley*, *Cross-Polarized C-band Scatterometer Measurements of the Sea Surface in Extreme Winds*, mdc.coaps.fsu.edu/scatterometry/meeting/docs/2016/Wed_AM/IOVWST_2016_Sapp.pdf
- [36] Alpers W, Zhang B, Mouche A, Zeng K, Wai Chan P (2016) Rain footprints on C-band synthetic aperture radar images of the ocean - Revisited, Remote Sensing of Environment, Volume 187, 15 December 2016, Pages 169-185, ISSN 0034-4257, dx.doi.org/10.1016/j.rse.2016.10.015.
- [37] Chou, K.-H., C.-C. Wu, and S.-Z. Lin (2013), Assessment of the ASCAT wind error characteristics by global dropwindsonde observations, J. Geophys. Res. Atmos., **118**, 9011-9021, dx.doi.org/10.1002/jgrd.50724.
- [38] Koch, W. (2004), Directional analysis of SAR images aiming at wind direction, IEEE Transactions on Geoscience and Remote Sensing **42**(4), 702-710, dx.doi.org/10.1109/TGRS.2003.818811.
- [39] Stoffelen, A., J. A. Verspeek, J. Vogelzang and A. Verhoef, "The CMOD7 Geophysical Model Function for ASCAT and ERS Wind Retrievals," *IEEE J. Sel. Topics in Applied Earth Observ. and Rem. Sens.* **10** (5), 2123-2134, May 2017. doi: 10.1109/JSTARS.2017.2681806.
- [40] Verhoef, A., J. Vogelzang, J. Verspeek and A. Stoffelen, "Long-Term Scatterometer Wind Climate Data Records", *IEEE J. of Sel. Topics in Applied Earth Observ. and Rem. Sens.* **10** (5), 2186-2194, May 2017, doi: 10.1109/JSTARS.2016.2615873.
- [41] Wentz, F. J., L. Ricciardulli, E. Rodriguez, B. W. Styles, M.A. Bourassa, D.G. Long, R.N. Hoffman, A. Stoffelen, A. Verhoef, "Evaluating and Extending the Ocean Wind Climate Data Record", *IEEE J. Sel. Topics in Applied Earth Observ. and Rem. Sens.* **10** (5), 2165-2185, May 2017, doi: 10.1109/JSTARS.2016.2643641.

- [42] Pineau-Guillou, L., Ardhuin, F., Bouin, M.-N., Redelsperger, J.-L., Chapron, B., Bidlot, J.-R. and Quilfen, Y. (2018), *Strong winds in a coupled wave-atmosphere model during a North Atlantic storm event: evaluation against observations*, Q.J.R. Meteorol. Soc. doi:10.1002/qj.3205.
- [43] Thomas, B.A., E.C. Kent, V.R. Swail, *METHODS TO HOMOGENIZE WIND SPEEDS FROM SHIPS AND BUOYS*, Int. J. Climatol. 25: 979–995 (2005), doi:10.1002/joc.1176.
- [44] Bigorre, S.P., R.A. Weller, J.B. Edson, and J.D. Ware, 2013: A Surface Mooring for Air–Sea Interaction Research in the Gulf Stream. Part II: Analysis of the Observations and Their Accuracies. *J. Atmos. Oceanic Technol.*, **30**, 450–469, doi: [10.1175/JTECH-D-12-00078.1](https://doi.org/10.1175/JTECH-D-12-00078.1).
- [45] Edmond M., D. Vandemark, J. Forsythe, A. J. Plueddemann and J. T. Farrar, 2012: Flow distortion investigation of wind velocity perturbations for two ocean meteorological platforms. Woods Hole Oceanographic Institution Tech. Rep. WHOI-2012-02, 66 pp.
- [46] Kloe, J. de, A. Stoffelen and A. Verhoef, "Improved Use of Scatterometer Measurements by Using Stress-Equivalent Reference Winds, *IEEE J. Sel. Topics in Applied Earth Observ. and Rem. Sens.* 10 (5), 2340-2347, May 2017, doi: 10.1109/JSTARS.2017.2685242.
- [47] Wang, Z., A. Stoffelen, C. Zhao, J. Vogelzang, A. Verhoef, J. Verspeek, M. Lin, and G. Chen (2017), *An SST-dependent Ku-band geophysical model function for RapidScat*, *J. Geophys. Res. Oceans*, 122, 3461–3480, doi:[10.1002/2016JC012619](https://doi.org/10.1002/2016JC012619).
- [48] Hasager, C.B.; Stein, D.; Courtney, M.; Peña, A.; Mikkelsen, T.; Stickland, M.; Oldroyd, A. Hub Height Ocean Winds over the North Sea Observed by the NORSEWInD Lidar Array: Measuring Techniques, Quality Control and Data Management. *Remote Sens.* **2013**, *5*, 4280-4303.
- [49] Stoffelen, A., et al., "Scientific Developments and the EPS-SG Scatterometer" *IEEE J. of Sel. Topics in Applied Earth Observ. and Rem. Sens.* 10 (5), 2086-2097, May 2017, doi: 10.1109/JSTARS.2017.2696424
- [50] P. Hoogeboom, 2018, DopSCAT capabilities update, Note dd. 27/2/2018, CITG, Technical University Delft, the Netherlands, available from Ad.Stoffelen@knmi.nl.
- [51] Bidlot J., D. Holmes, P. Wittmann, R. Lalbeharry, and H. Chen Intercomparison of the performance of operational ocean wave forecasting systems with buoy data *Wea. Forecasting*, vol. 17, 287-310, 2002.
- [52] Haseler, J., 2004, 'The early-delivery suite', ECMWF Tech. Memo. 454, Fig. 3, www.ecmwf.int/sites/default/files/elibrary/2004/9793-early-delivery-suite.pdf.
- [53] Vogelzang, J., A. Stoffelen, R. D. Lindsley, A. Verhoef and J. Verspeek, "The ASCAT 6.25-km Wind Product", *IEEE J. of Sel. Topics in Applied Earth Observ. and Rem. Sens.* 10 (5), 2321-2331, May 2017, doi: 10.1109/JSTARS.2016.2623862.
- [54] Vogelzang, J., and A. Stoffelen, "ASCAT Ultrahigh-Resolution Wind Products on Optimized Grids", *IEEE J. of Sel. Topics in Applied Earth Observ. and Rem. Sens.* 10 (5), 2332-2339, May 2017, doi: 10.1109/JSTARS.2016.2623861.
- [55] I.L. Wijnant, A. Stepek, M. Savenije and H.W. van den Brink, User manual of the (KNMI North Sea Wind) KNW-atlas, Version 9: June 2016, <http://projects.knmi.nl/knw/User%20manual-versie9.pdf>.
- [56] University of Rhode Island, Hurricanes: Science and Society, www.hurricanescience.org/science/observation/satellites/quikscat/.
- [57] Wikipedia, Cyclone Numa, en.wikipedia.org/wiki/Cyclone_Numa.

1.4. Acronyms

ASAR	Advanced SAR (on ENVISAT)
ASCAT	Advanced Scatterometer on MetOp
AWDP	ASCAT Wind Data Processor
C band	Microwave band around 5 cm wavelength
Cal/Val	Calibration and Validation
CDR	Climate Data Record
CEOS	Centre for Earth-Observing Satellites
CFOSAT	Chinese French Ocean Satellite
CMEMS	Copernicus Marine Environment Monitoring Service
CNES	Centre national d'études spatiales (France)
CERSAT	Centre ERS Archivage et Traitement
CSIC	Agencia Estatal Consejo Superior de Investigaciones Científicas
CUDA	Compute Unified Device Architecture
DOFT	Department of Physical and Technological Oceanography
DR	Data Repository
DUE	Data User Element (ESA)
ECMWF	European Centre for Medium-range Weather Forecasts
ENVISAT	ESA Environmental Satellite with SAR (2002-2012)
EPS	EUMETSAT Polar System
ERC	European Research Council
ERS	European Remote-sensing Satellite (global mission: 1991-2000)
ESA	European Space Agency
ESTEC	ESA Science and Technology Centre
ETC-P3	Extra-Tropical Cyclone P3 aircraft campaign in 2016
EU	European Union
FP	Final Presentation
GMES	Global Monitoring for Environment and Security (now EU Copernicus)
GNSS-R	Global positioning system signals reflected on the ocean surface
GMF	Geophysical Model Function
HH	Horizontal co-polarization
HV	Cross polarization; horizontal to vertical
HY2A	Chinese pencil-beam scatterometer 2011-2015
IFREMER	L'Institut Français de Recherche pour l'Exploitation de la Mer
IOVWST	International Ocean Vector Winds Science Team
ISRO	Indian Space Research Organisation

ITT	Invitation To Tender
JASON	Serltimeters (since 2001)
JPL	Jet Propulsion Laboratory (NASA)
KNMI	Koninklijk Nederlands Meteorologisch Instituut
KO	Kick Off
L1	Calibrated and geocentered measurements on instrument coordinates
L2	Geophysical instrument-swath record
L3	Geophysical instrument record on geographical grid
L4	Record on geographical grid, merged from different data sources
MetOp	Currently Operational Meteorological satellite from EUMETSAT
MLE	Maximum Likelihood Estimator
MTR	Mid-Term Review
NASA	National (USA) Aeronautics and Space Administration
NCAR	National (USA) Center for Atmospheric Research
NESZ	Noise-Equivalent Sigma Zero
NOAA	National (USA) Oceanographic and Atmospheric Administration
NRCS	Normalized Radar Cross Section (also Sigma Zero)
NSCAT	NASA Scatterometer (1996-1997)
NWP	Numerical Weather Prediction
OMI	Ozone Monitoring Instrument
OS	Operating System
OSI SAF	Ocean and Sea Ice SAF
OSVW	Ocean Surface Vector Wind
PDGS	Payload Data Ground Segment
PDF	Probability Distribution Function
PI	Principal Investigator
QuikScat	NASA pencil-beam scatterometer with swath mission from 1999-2009
R&D	Research and Development
RA	Radar Altimeter
RadarSat	Canadian satellite with SAR
RAM	Random Access Memory
RFSCAT	Rotating Fan-beam Scatterometer
RR	Rain Rate
RS2	RadarSat-2
S	Software
S1	Sentinel 1
SAF	Satellite Application Facility

SAG	Science Advisory Group
SAR	Synthetic Aperture Radar
SCA	Scatterometer on board MetOp-SG
SFMR	Stepped-Frequency Microwave Radiometer
SG	Second Generation
SHOC	Tropical Satellite Hurricane Observation Campaign in 2016
SMOS	Soil Moisture and Ocean Salinity
SoW	Statement of Work
TO	Start time of CHEFS
TD	Test Data set
TEC	Total Electron Content
TN	Technical Note
TOPEX	TOPOgraphy Experiment (altimeter TOPEX/Poseidon starting 1992)
SSM/I	Special Sensor Microwave Imager
TU	Technical University
VH	Cross polarization; vertical to horizontal
VTEC	Vertical TEC
VV	Vertical co-polarization
WBS	Work Breakdown Structure
WMO	World Meteorological Organisation
WP	Work Package
WPD	WP Description
WVC	Wind Vector Cell
X band	Microwave band around 3 cm wavelength

2. State of the art in ocean wind sensing

2.1. C-band radar

The scatterometer and Synthetic Aperture Radar (SAR) are both satellite radar instruments, which provide a measure of wind speed and/or direction near the sea surface. The European development of scatterometer and SAR processing software for operational use in weather and marine forecasting is coordinated in an international context through projects such as the EUMETSAT Ocean and Sea Ice Satellite Application Facility (OSI SAF), the EUMETSAT Numerical Weather Prediction SAF (NWP SAF), the EUMETSAT Advanced Retransmission Service (EARS), EU Copernicus Marine Environment Monitoring Service (CMEMS), EU projects and ESA projects. ASCAT measures co-polarized (VV) polarized C-band backscatter in three azimuth directions [1] and provides reliable high ocean-surface vector wind (OSVW) information in open ocean and marine coastal regions from C-band scatterometers, where generally limited in situ measurement capability exists.

The KNMI team processes winds from scatterometers on board the past ESA ERS satellites (AMI) and QuikSCAT (SeaWinds) mission from NASA/NOAA, the current MetOp (ASCAT-A and ASCAT-B) from EUMETSAT, and is involved in past, existing and future missions from India and China, in particular OceanSat-II/III, ScatSat, HY-2A/B and CFOSAT. Operational products that have been developed at KNMI include 12.5-km and 25-km ASCAT winds over the open ocean, where the former provides winds in coastal areas as well. Wind scatterometry is well established and used in manifold applications [1-19]. Nominal scatterometer winds are calibrated against moored buoys [1,2,3,5,6,8,13] and extensively used to validate NWP models (e.g., www.nwpsaf.org). Scatterometers are very stable and thus reliable instruments [30].

The ASCAT stability of about 0.03 dB [30]¹, makes it possible to obtain extreme winds at high quality, i.e., well calibrated. Moreover, the low random error, typically 0.2 dB, on each of the backscatter values, makes it possible, after combining the backscatter triplet in the wind retrieval to obtain a further noise reduction by a factor of about 1.7. Using the current CMOD7 Geophysical Model Function (GMF) [39], we note that a 0.1 dB uncertainty at a modal wind speed of 7 m/s corresponds to about 0.1 m/s wind speed uncertainty. However, at 40 m/s wind speed, due to the saturation of the VV GMF, 0.1 dB corresponds to about 4 m/s error. Through CHEFS, we thus may obtain a calibration certainty of about 1 m/s at 40 m/s, corresponding to the instrumental stability of ASCAT. Such value would be unprecedented and is not obtained by any other satellite retrieval to our knowledge. However, the error analysis for wind data derived from space-borne sensors requires special care due to non-linearities and ambiguities in the GMF leading to multiple solutions in the wind retrieval [16].

2.2. SCA instrument

The Scatterometer (SCA) is one of the high priority EPS-SG payload instruments planned to be on the Metop-SG B series. It is the follow-on of the Metop Advanced Scatterometer (ASCAT) series. SCA will provide ocean surface vector wind (OSVW) observations and additional information on soil moisture, vegetation, thaw, sea ice and sea ice drift, which constitutes an important input to all mandated EUMETSAT applications of nowcasting, global and regional Numerical Weather Prediction (NWP), oceanography, hydrology and climate monitoring and research [49].

¹ Note that the stability specification of ASCAT is much less constrained at 0.20 dB.

The SCA instrument is a real-aperture C-band, pulsed imaging radar with six fixed fan beam antennas, three on both sides of the satellite ground-track. All antennas emit in vertical polarization. The 4 side antennas receive only vertically polarized signals, whereas the 2 mid antennas can emit H-polarized signals and receive both V and H-polarized signals. Following ASCAT configuration, the principal elevation planes of the SCA antenna beams are oriented at 45° (Fore-left), 90° (Mid-left), 135° (Aft-left), 225° (Aft-right), 270° (Mid-right) and 315° (Fore-right) with respect to the flight direction. The major improvements to be brought by SCA with respect to ASCAT are:

- the baseline spatial resolution of 25 km x 25 km,
- the radiometric stability of ≤ 0.1 dB,
- the addition of VH and HH polarization measurements on the mid beams.

The latter improvement is mainly added for the objective of tracking extreme weather events. In the design of SCA, cross-polarization (VH) capability was decided after investigation of its behavior with RadarSat SAR acquisitions with respect to the better known co-polarization (VV and HH) responses [31,32,33]. It has been demonstrated that VH radar backscatter signals remain sensitive at very high to extreme wind conditions see, e.g., [30-32]. This addition is a key one in the context of this study.

In addition, Doppler capability may be obtained on SCA, which would be useful for obtaining wind direction information in hurricanes [50].

2.3. SAR reference data

The Copernicus Sentinel-1 (S1) mission provides continuity of C-band Synthetic Aperture Radar (SAR) operational applications and services in Europe. The mission builds on the SAR experience with the ERS and Envisat SAR instruments. The S1 mission is a two-satellite constellation, with four nominal operational modes on each spacecraft designed for maximum compliance with user requirements. Level-2 products consist of geo-located geophysical products derived from Level-1. Level-2 Ocean (OCN) products for wind, wave and currents applications contain the following geophysical components derived from the SAR data:

- Ocean Wind field (OWI);
- Ocean Swell spectra (OSW);
- Surface Radial Velocity (RVL).

Although both Sentinel-1 A and Sentinel-1B are orbiting Earth in the same orbital plane and provide complementary coverage, the operation modes allow only that they cover the whole globe once every six days. The C-band SAR instrument on board Sentinel-1 A has two modes to enable dual-polarization measurements with large swaths: Extra Wide (EW) and Interferometric Wide (IW) swath modes. Dual polarization acquisitions are VV and VH or HH and HV, see e.g., [33,31], but these are made only part of the time, further complicating the targeting of hurricanes. We further note that the calibration accuracy and stability of SAR systems is typically 0.5 dB and lower than that of a scatterometer. At 40 m/s and VV polarization, this implies a wind reference calibration accuracy of about 20 m/s, rendering SAR data rather poor in resolving high winds. In particular, Noise Equivalent Sigma Zero (NESZ) corrections are visible in many SAR images, e.g., [31]. Nevertheless, S1 SAR data will be a very useful addition to ENVISAT, Chinese GF-3 and RadarSat-2 SAR in CHEFS and beyond to prepare for SCA processing in extreme winds.

2.4. Other satellite sensors

Besides C-band radar, other wavelengths may be exploited to obtain winds over sea. Ku-band scatterometers are plentiful, while these suffer from ancillary geophysical effects, such as rain and

SST, due to the shorter wavelength. Nevertheless, they usually measure both VV and HH co-polarization, where HH polarization features enhanced sensitivity for extreme winds at the higher incidence angles (though less than VH). X-band SAR systems are in space too. Radiometers are providing wind speed (SSM/I) and wind direction at high speeds (WindSat) by combining different microwave channels, but suffer from contamination by the wet atmospheric contributions, which contribute uncertainty in extreme weather conditions. Both active and passive L-band satellite instruments have been flown, where the longer wavelengths are not sensitive to the atmosphere and may provide sensitivity to extreme winds.

However, measuring extreme winds from space is challenging as calibration is needed and calibrated in situ reference winds are scarce. On the other hand, theoretical statistical descriptions of the high-wind ocean surface, where patchy foam, droplets, spume and wave breaking occur are much simplified, while the microwave interaction on cm scales is rather complex too. Theoretically-based models typically obtain accuracies of about 1 dB, which is often not very useful in measuring extreme winds. The development of Geophysical Model Functions for wind scatterometer OSVW has therefore been based on empirical methods, using moored buoys as absolute reference [2].

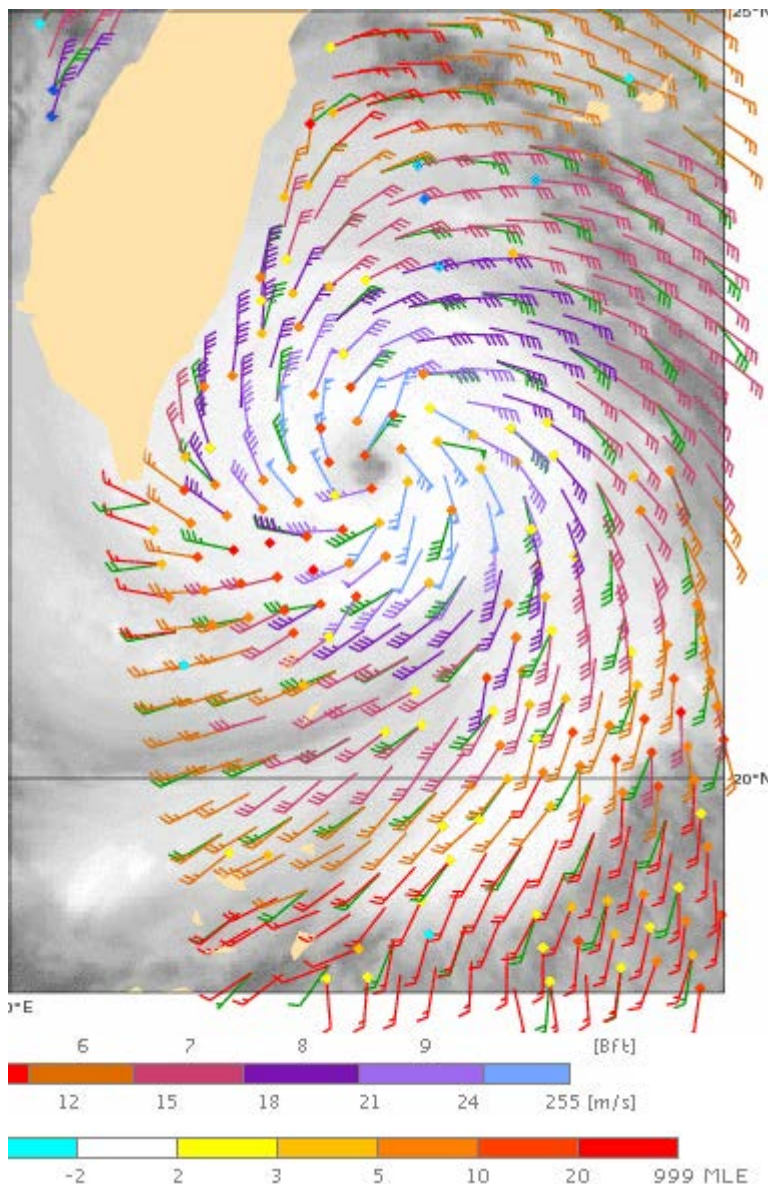


Figure 2.1: An example of measured ASCAT scatterometer hurricane winds, explained at http://projects.knmi.nl/scatterometer/tile_prod/tile_app.cgi. Winds up to 70 knots or 35 m/s are measured by ASCAT in speed-coloured flags for this case, while the collocated ECMWF winds are plotted in green.

3. Wind references

3.1. Wind calibration references for high and extreme OSVW

Typhoons cause much havoc in the tropical waters, where its winds are devastating and occasionally cause water levels to surge to catastrophic heights. A particularly pressing requirement in the OSVW community is therefore to obtain reliable extreme winds in hurricanes (> 30 m/s) from scatterometers, since extreme weather classification, surge and wave forecasts for societal warning are a high priority in nowcasting and NWP.

Moored buoy winds have been used in the EUMETSAT SAFs as an absolute reference to produce calibrated scatterometer data [39]. Moored buoys are perceived as accurate measurements with small bias (< 0.1 m/s) and good accuracy (< 0.5 m/s). One reason for the good performance is the dedicated design for wind measurement, such that wind flow acceleration or deceleration due to measurement platform interference is generally minimal ($< 5\%$ [44,45]). Unfortunately, moored buoy data are geographically biased and sparse and a year of collocation data is needed to arrive at statistically significant calibration results. On the other hand, for ASCAT-A and -B more than a decade of collocations is now available with many winds above 15 m/s.

Independent winds from a short-range Numerical Weather Prediction (NWP) model may also serve as wind reference and these are available at any observation location and time for satellite and buoy collocation. This allows both triple collocation analysis [3] and extensive NWP comparison to better define in situ, satellite and NWP wind errors [46,47]. Note that spatio-temporal biases of such NWP forecasts are monitored closely in order to provide a good (relative) wind reference.

However, for very high and extreme winds above 25 m/s, moored buoys are not reliable either and collaboration has been sought with the NOAA hurricane hunters. Moreover, controversy exists in the OSVW satellite community on the quality of moored buoys above 15 m/s rather than 25 m/s; see figure 3.3. This needs further investigation.

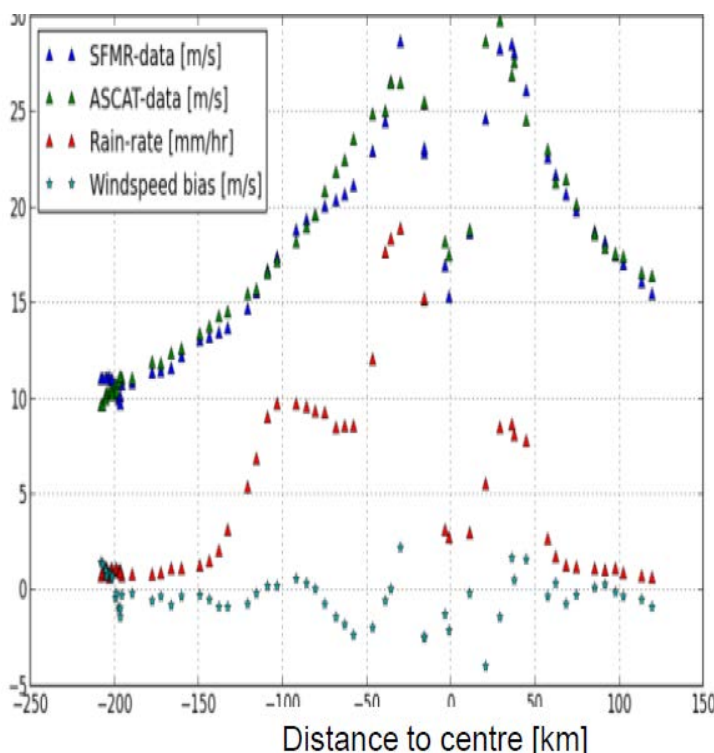


Figure 3.1. Illustration of modified (2012) SFMR wind speeds (blue), rain rate, RR, (red) and collocated ASCAT speed, V, (green) and SFMR-ASCAT speed difference. SFMR speeds have been ad hoc modified to match ASCAT over a large number of typhoons. This matching required subtraction of $\ln(RR)$ and $\ln(V)$ and provides an estimate of current typical calibration uncertainty. Although uncertain, the ASCAT depiction of typhoon structure appears generally faithful up to 35 m/s.

3.2. NOAA hurricane hunters

The NOAA hurricane hunters go into hurricanes to drop sondes, and thus obtain wind profiles in the lowest few kilometers of hurricanes, and mounted dedicated microwave instrumentation on aircraft, to obtain detailed wind patterns in hurricanes, such as the Stepped-Frequency Microwave Radiometer (SFMR). Ideally, local dropsonde winds may be statistically used to calibrate SFMR as they have similar spatial representation (“footprint”), which in turn, after spatial aggregation to scatterometer footprints, is used to calibrate satellite scatterometers and radiometers in overflights. Given the scale of hurricanes and the footprint of radiometers and scatterometers, satellite typhoon speeds are expected to be less extreme than in-situ measured extremes, due to the implicit spatial aggregation of the satellite-based winds. This is particularly aggravated by the relatively narrow dimensions of the tropical hurricane eye wall. The calibrated spatial wind patterns measured by SFMR may however be aggregated to approximately match the satellite footprints and thus provide a calibration reference and an estimate of local wind variability (see Fig. 3.1). Although this approach is credible in principle and physically more consistent than any other global method to obtain maximum winds in hurricanes, research is ongoing to understand the exact physical interpretation of drop-sonde winds and SFMR in the inherently extremely variable conditions in tropical hurricanes and to obtain more hurricane flight data. Since processing artefacts are known to exist for both dropsondes and SFMR, at an IOVWST high winds meeting, NOAA agreed to reprocess the dropsondes and SFMR to provide a more accurate reference [35]. The reprocessing of the dropsondes is ready, while SFMR reprocessing is being finished (Zorana Jelenak, personal communication).

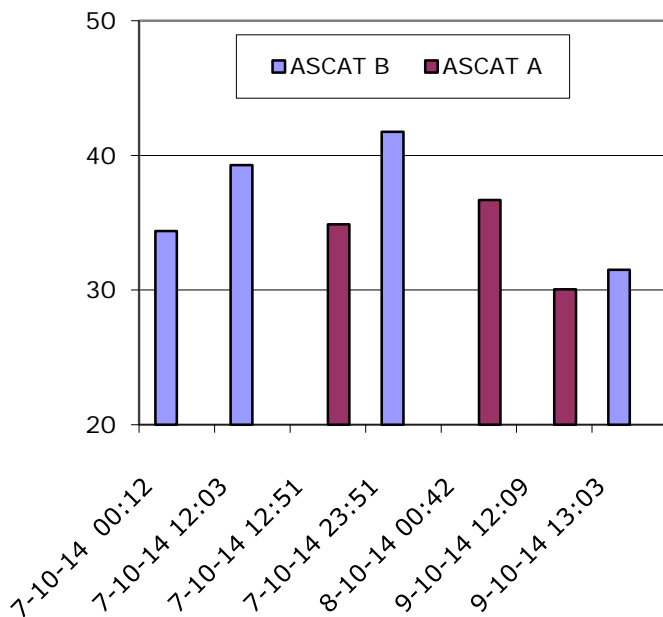


Figure 3.2: ASCAT acquisitions of maximum wind early October 2014 up to 42 m/s (150 km/h). ASCAT-A appears low as compared to ASCAT-B due to the 2014 calibration bias of ASCAT-B minus ASCAT-A of ~0.1 dB, where required accuracy is 0.2 dB (which nominally corresponds to ~0.2 m/s). Due to VV GMF saturation, 0.1 dB at 40 m/s is about 4 m/s. For extremes additional capability and/or more careful instrument calibration is needed [30].

As mentioned above, capabilities in hurricane winds motivated for SCA the addition of a VH channel. It also motivated ESA to provide the hurricane hunters on plane Ms. Piggy with a VH scatterometer antenna panel, which is now mounted and first measurements generally confirm the VH GMF behavior at extreme speeds as derived from RadarSat [35]. The forthcoming winter and summer hurricane flight campaigns, will provide further VH and collocated ancillary observations in the years to come. Where in situ measurements are generally unreliable and hazardous, the NOAA “hurricane hunter” campaigns collect data that may be used to calibrate scatterometer winds in extreme conditions [20].

3.3. Other high-wind sources

Wind information over the oceans is also available from in-situ measurements by platforms, ships and buoys, analysis from Numerical Weather Prediction (NWP) models, and remotely sensed by passive and active microwave space-borne sensors. It is important to consider the different spatial and temporal sampling characteristics, as well as the different error statistics, when comparing wind data from these sources. Vandemark et al. compared wind mast measurements to a moored buoy and found no biases up to 25 m/s, confirming earlier observations. They also found that scientific references claiming that buoy winds are probably affected by wave effects to be based on NWP model studies and therefore unreliable [13]. In CHEFS we will need to seek observational evidence of the quality of the different wind observing systems at high and extreme winds in order to obtain a reliable in situ wind reference.

Indeed, all satellite-based winds suffer from a lack of calibration, due to the lack of a consolidated wind reference. NWP winds have no absolute calibration, but are usually well monitored and therefore may be regarded as an effective relative standard of comparison and collocation, since NWP winds are available at any time and location, much unlike in situ references which are generally sparse.

Platform winds exist, for example, in the Gulf of Mexico and North Sea, that experience hurricane-force winds occasionally [42]. However, measuring representative winds on a platform is quite challenging due to wind flow distortions by the platform. Winds measured on a platform (extension) could be both higher or lower than the undisturbed wind and disturbed winds tend to be more variable than undisturbed winds at the same location [48]. Even when the enhanced variability due to platform is accounted for, it is difficult to exclude systematic biases, hence calibration using platform winds is complex. Another problem is that platform winds are usually measured at 60m or higher and where a simplified downscaling rule is used to obtain winds at 10m height. Downscaling may be prone to biases too.

For winds measured on ships, similar concerns exist as for platform winds. However, dealing with ship winds is more complex, as ships move, thereby modifying both measurement height and distortion [43]. [43] reports on a random observational error variance of collocated ship and moored buoy data of around resp. 1.4 and 2.3 m/s. Again, the more than double random variability in ship winds is rather concerning, as there is little guarantee that the processes leading to this variability do not introduce speed-dependent biases, which may be quite unpredictable at the extremes. [43] also reports about visual wind estimates, which generally have larger errors than corrected anemometer ship winds and are not further considered here.

3.4. Comparing extreme wind data

As outlined above, obtaining unbiased wind reference data appears a challenge. When such data have been collected, a next step is to compare other data sources to the calibration reference. Usually, different data sources do not have identical geophysical, spatial and temporal aggregation and therefore associated uncertainties have to be accounted for in the calibration process. Noise broadens probability distribution functions of true variables, hence more extreme values will appear. For example, [3] discusses how random errors, e.g., due to spatial (and temporal) representation and flow distortion, may cause biases in case of conditional sampling, see Figure 3.3. Due to the exponential nature of speed PDFs, the largest artificial speed biases occur at high speeds.

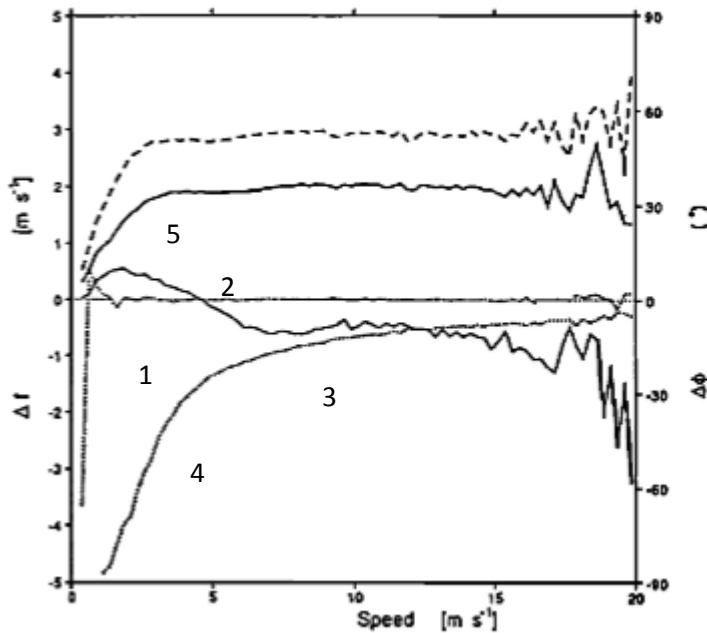


Figure 3.3: Simulated wind speed and direction difference statistics of X minus Y as a function of average wind speed, $(X+Y)/2$, for a global true wind speed distribution. The simulation is done with a scatterometer global wind distribution as "truth" and added wind component standard errors of 1.0 and 1.8 ms^{-1} for X and Y, respectively. Speed bias (thin solid line, 1), standard deviation (thick solid line, 2), direction bias (thin dotted line, 3), standard deviation (-ve, thick dotted line, 4), and vector root-mean-square (dashed line, 5) of differences are shown. © [3]

Clearly, all bias in Figure 3.3 is caused by binning of the wind variables (conditional sampling) against a simulated noisy variable $X+Y/2$. All errors are unbiased and normal and in this case Y winds will be more extreme than X winds, due to the larger random noise variance. This is similar to, for example, a ship anemometer sensing random wind variations due to flow distortion and motion, which is not present in a collocated moored buoy and hence the ship will provide larger extreme values.

Besides geophysical representation and measurement noise, another relevant aspect in comparisons resides in the spatial and temporal representation. In particular, hurricane winds are gusty and wind extremes depend on temporal aggregation. For example, the National Hurricane Centre (NHC) uses 1-minute sustained maximum winds for hurricane classification and public warning. Using Taylor's hypothesis to exchange the time and space coordinates, a 1-minute sustained 60 ms^{-1} wind corresponds to a distance of 3.6 km. Scatterometers may resolve wind on the 20-km scale over typically 5 minutes and therefore do not resolve the gustiness of 1-minute sustained winds in time nor space. Given the random variability on all turbulent scales, the scatterometer will miss out on the variability on the smallest scales and therefore will deliver hurricane winds that are less extreme than 1-minute sustained winds. The knowledge of this difference is obviously relevant, as it guides the capability of scatterometers to contribute to the determination of hurricane categories. The use of gustiness guidance information is operational practice in nowcasting and may be further verified from the SFMR or SAR instrument data. Moreover, the associated information on spatio-temporal variability in hurricanes is needed to calibrate satellite instrument footprint data to point-measurement wind references, such as dropsondes or moored buoys.

3.5. The inconsistency of high and extreme wind references

To avoid biases due to flow distortion by the measurement platform and due to platform motion, moored buoys appear the most suitable candidate to serve as a wind reference. However, moored buoys are not suitable as wind reference in extreme wind conditions, due to the extreme sea states that will occur, particularly for speeds above 25 ms^{-1} . In this regime dropsondes appear a good wind reference, as these are not effected by platform issues. Dropsondes however may drift, sample regularly, but at unpredictable heights, and their path may be systematically affected by the hurricane structure.

It is of paramount importance to analyse how these two in situ references may be combined in a continuous in situ wind reference that can be used for wind calibration. In Figure 3.4 dropsonde speeds are compared to ASCAT speeds (a), moored buoy speeds to ASCAT speeds (b) and ASCAT speeds to ECMWF short-range forecast speeds (c). For (b) and (c), it is no surprise that a good match is obtained, as moored buoys have been used as a reference in both the development of the ASCAT GMF and the ECMWF model. However, it is disturbing that dropsonde winds appear much higher than ASCAT speeds for speeds of 15 ms^{-1} and higher. If both dropsonde and moored buoy speeds are to be used as calibration reference, then their characteristics will need to be consolidated in one way or the other.

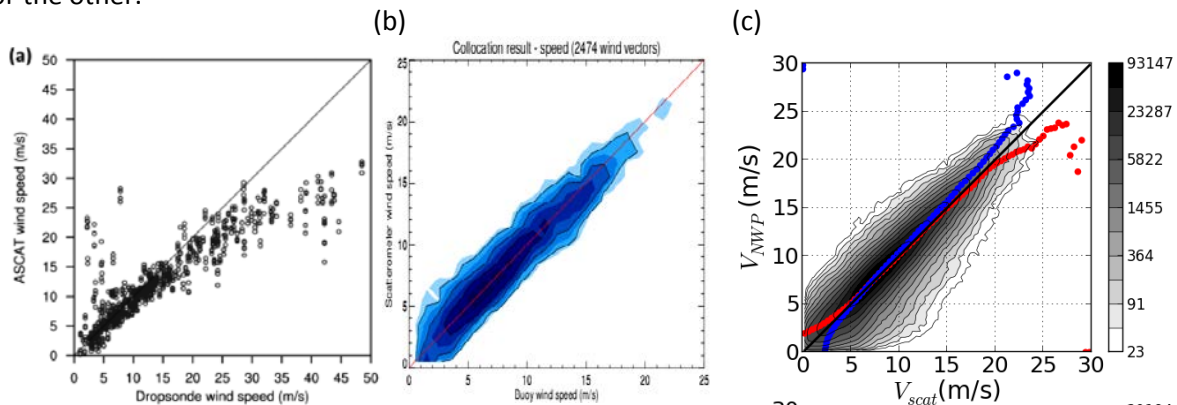


Figure 3.4: ASCAT wind speed scatter plots of a) ASCAT versus drop sondes (from [37]), b) ASCAT versus moored buoy winds and c) ECMWF NWP winds versus ASCAT. Using drop sondes, moored buoy winds and NWP references above 15 m/s may result in discrepancies due to height and position representation differences.

3.6. User requirements

A main motivation in CHEFS is to provide calibrated scatterometer winds in the EPS SG era. At that time, NWP models will have evolved and be more often used for high-resolution nowcasting of hurricanes, using inputs from an increasing number satellite instruments, notably scatterometers from the CEOS OSW constellation, contributed by Europe, India, China and Russia, among others. In addition, a constellation of microwave radiometers and research missions will be providing ocean surface wind speed information probably.

It is clear that prospective user requirements from the various application areas (nowcasting, NWP, oceanography, climate) for a continuous and consistent calibration wind speed reference will become urgent, when wind information from NWP and satellite references will more and more dominate the weather advisories and meteorological and oceanographic research.

4. The next steps for obtaining calibrated extreme satellite winds

The CHEFS project has been defined for the further understanding of satellite remote sensing of high and extreme wind conditions over the ocean, more in particular for high and extreme wind retrievals from C-band scatterometer missions, such as SCA. The first step in obtaining calibrated extreme satellite winds is clearly in consolidating the in situ wind references. Also, the characterization of spatial scaling issues, spatial representation, and related consequences for product sample resolutions and validation approaches must be addressed. Finally, the evolution of the current ASCAT operational wind services to more reliable extreme winds with SCA, using the various polarization options, will be elaborated and summarized.

4.1. Approach for moored buoy reference

As motivated in section 3, we focus on moored buoys, as we found them to be the most reliable (least scatter against collocated references). Analysis of the wind characteristics of different types of moored buoys in terms of height and mooring, as used in triple collocation analyses, will be performed, inter alia, against ECMWF and ASCAT wind references.

Among others, the International Comprehensive Ocean-Atmosphere Data Set (ICOADS; icoads.noaa.gov/) offers surface marine data, which are freely distributed worldwide. The ICOADS records contain most metadata, but where ICOADS winds are 10-minute values “super-obbed” into hourly values. Note that hourly values at 50 ms^{-1} correspond to a spatial average over 180 km, extending much beyond a 25-km scatterometer WVC. Alternatively, archived data from the WMO Global Telecommunication System (GTS) may be used in developing a wind reference. While GTS data are 10-minute values, only one value is reported every hour. Since the high time resolution will help reduce representation error, the GTS data is favored for CHEFS, rather than the super-obbed ICOADS.

Further analyses of off-line and GTS sources learns that many more GTS moored buoy winds are available than off-line and therefore our chances of encountering extremes will be higher; see Figure 4.2. Over 2009-2014, the GTS set encounters over 100 times winds of 25 ms^{-1} and higher. We moreover found that off-line winds that do not appear in the GTS set, are rarely above 15 ms^{-1} . Finally, ECMWF established a procedure to blacklist on a monthly basis those GTS stations that provide disrupted, constant or otherwise erroneous data [51]. In figure 4.1 collocated off-line and GTS winds, resp. as delivered by the archive portals and ECMWF (MARS), are compared in order to verify that they will result in the same wind reference. The time averaging and sampling difference is probably causing most of the scatter with standard deviation of 0.4 ms^{-1} . There may be several reasons for the small overall bias, but in the light of the accuracy of the calibration effort that we pursue for high and extreme winds, the 0.1 ms^{-1} bias is assumed negligible.

The asymmetry in outliers in Figure 4.1 is annoying as it can change the mean, while most points may in fact agree, i.e., are symmetrically and closely distributed around the diagonal. A QC test may be tested and applied to discard points/stations well separated from the diagonal.

An expressed main concern is that moored buoys do not function properly in high sea state. Collocation with model wave data may segregate any measured speed of a given buoy type in relatively high, modal or low sea state to analyze anomalous behavior against ECMWF and/or scatterometer references.

Statistics may be first aggregated by buoy, then sorted by buoy type, sensor height and sea state condition, inter alia, in order to analyze and detect dispersion in the objective wind speed reference.

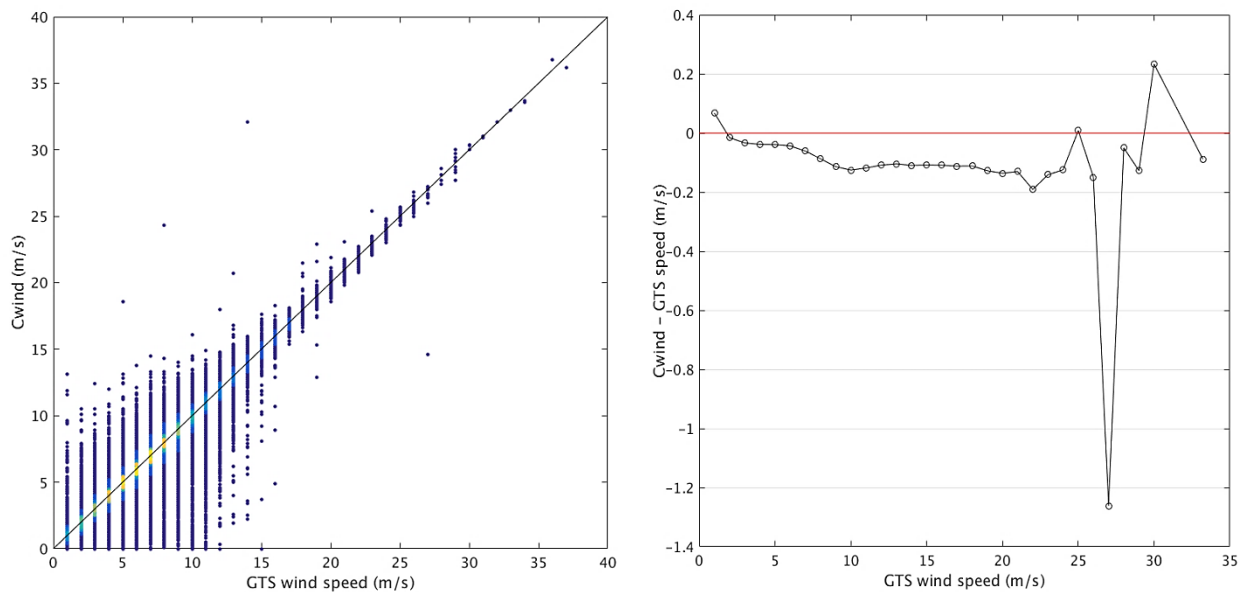


Figure 4.1: Archived buoy winds collected from NDBC, TAO, PIRATA and RAMA versus the same winds received in NRT over the WMO GTS (left) over 2009-2014. The scatter-density plot features colors on the scale, <1%, <10%, <20% ... <90% of the maximum bin value. Archive-GTS speed bias versus GTS-reported speed (right), which appears negligible. (courtesy, Wenming Lin, NUIST)

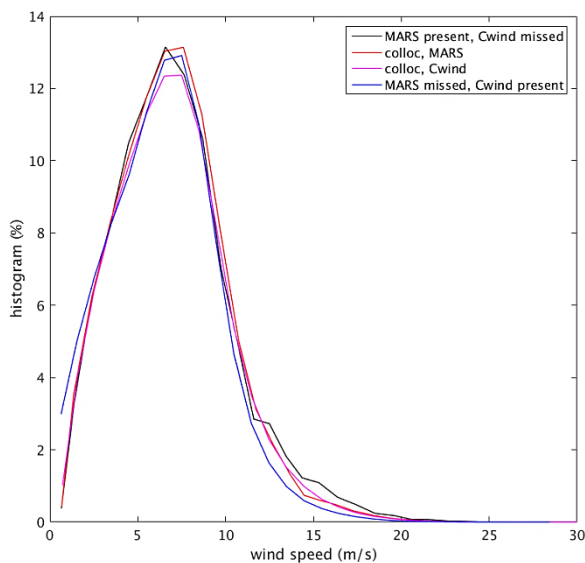


Figure 4.2: Wind speed PDF of archived buoy winds collected from NDBC, TAO, PIRATA and RAMA (Cwind), as collocated with the same data received by GTS at ECMWF (called MARS; purple), vice versa (red), Cwind PDF if no GTS found (blue) and vice versa (black). Red and purple are plotted in Figure 4.1. versus the same winds received in NRT over the WMO GTS (left). Archive-GTS speed bias versus GTS-reported speed (right), which appears negligible. Red and purple correspond to 3.2 million collocations, black to 3.3 million points and blue to 1.7 million. Collocation is successful when location, hour and heights match. (courtesy, Wenming Lin, NUIST)

4.2. Approach for dropsondes

The large collection of high wind cases (hurricanes, storms, cyclones) with dropsondes forms the basis for further assessments dedicated to the high and extreme winds conditions using dropsondes.

Dropsondes may be compared against SFMR and SAR on the local scale and with ASCAT and ERA5 on larger scales. In addition, also moored buoys may be compared to ASCAT and ERA5 as a function of wind speed, thus providing another in situ reference. In this way, the consistency of the in situ

references may be tested as in Figure 3.4. Direct comparisons of moored buoys and dropsondes are unlikely.

Dropsondes exist in different vertical sampling above the ocean, in different profile (shear) conditions and in different drift conditions and it will be of interest to segregate the dropsonde data into different height and quality categories. It appears clear from figure 3.4 that the scatter in dropsonde winds at 20 ms^{-1} ASCAT winds is relatively large and it will be necessary to understand this variability in the light of acquiring an accurate and consistent wind reference.

Since ASCAT retrievals have good relative accuracy around 20 ms^{-1} , they could be used as a (relative) reference to understand biases and scatter in both moored buoys and dropsondes. In addition, collocations of SFMR with moored buoys may exist occasionally to explore biases and scatter.

4.3. NWP reference

Another potential reference that may be used to compare to different wind observation types are NWP fields, notably ECMWF [31]. Operational winds are probably the most accurate today, but ECMWF implements a new model version regularly, which potentially impacts the wind reference as different parameterizations and dynamical model closure may be implemented. To avoid such NWP changes in time, short-range forecast winds from reanalysis may be used, such as from ERA5. The quality of ERA5 wind fields is comparable to the quality of operational ECMWF wind fields in 2013 (software.ecmwf.int/wiki/display/CKB/ERA5+data+documentation). Of course, the performance and thus extreme-wind climatology of ERA5 may be somewhat variable over the years, due to gradually changing observation inputs, but is expected to be a much more stable reference than the operational ECMWF winds. For the NWP reference to be independent of observed inputs, among which scatterometer data, short-range forecasts may be used. ERA5 is using only the so-called "delayed mode" suite [52], where the observation window overlaps the forecast range until +3 hours. So, if from the hourly forecast output +1 and +2 hours are ignored, then AWDP should only interpolate the forecasts after +3 hours range for ASCAT winds, which then will appear in the next ERA5 observation window, hence no overlap exists with the analysis observation window that was used to produce the forecasts used in AWDP. Therefore, the ERA5 forecasts are independent from the observations it will be compared with.

4.4. SAR data assessment

The collection of Canadian RADARSAT, ESA ENVISAT, the Chinese GF-3 and Sentinel-1 (S1) SAR missions and ASCAT extremes will be the basis of the collocation data with ancillary, in situ, campaign or NWP model data (short-range ERA5 forecasts of winds). Particular attention will be given to the quality of SAR calibration and noise for the various instruments.

Moreover, the consistency of SAR backscatter map characteristics is analyzed for extreme winds in comparison to ancillary hurricane data, e.g., SFMR, to consolidate the SAR inputs to the project. Inter alia, a comparison of SAR data and hurricane models is performed to obtain a better understanding of hurricane structure and wind variability in extreme conditions. Finally, as depicted in Figure 4.3, we segregate variable NRCS from homogeneous regions and analyze the effects on our diagnostics using SAR and ancillary data.

Comparisons with lower wind speeds, comparisons with published scientific literature, as well as sensitivity experiments to understand the influence of the various remote sensing or geophysical factors will be performed.

Using consistent S1 and RadarSat backscatter data, the KNMI synthesis of the C-band VH GMF may be extended to S1 acquisitions, using SFMR and ECMWF reference inputs, cf. [31].

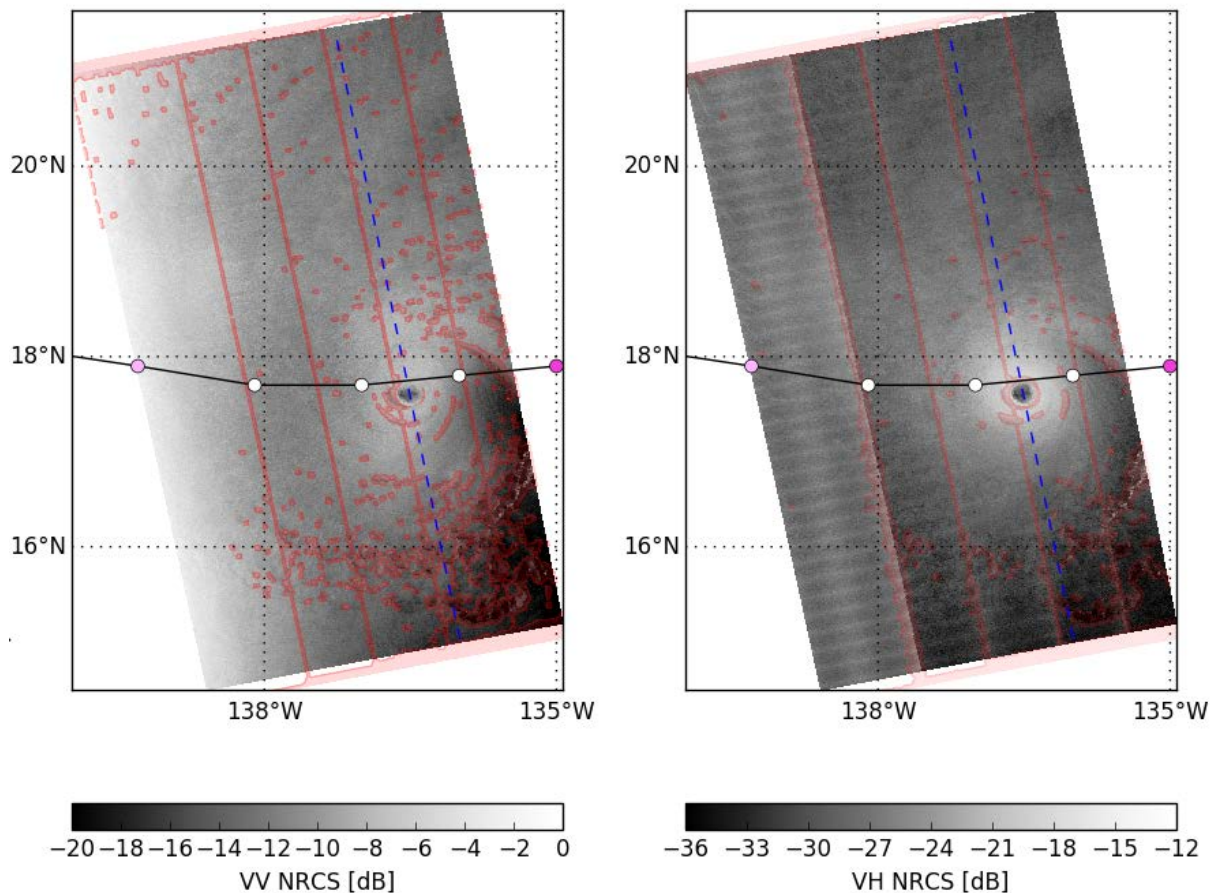


Figure 4.3: NRCS inhomogeneities (red encircled) detected by multi-resolution local gradient test in S1 SAR VV (left) and VH (right) images cf. [38].

4.5. Satellite wind reference

In order to obtain a better satellite wind reference, calibration of SFMR will be investigated using dropsondes and subsequently this wind reference will be used to tune the VV GMF by comparing ASCAT winds with reprocessed (by NOAA) and upscaled SFMR. The upscaling process further provides additional information on sub-WVC wind variability. This variability will be compared to the variability in SAR VH images for consistency. Information on sub-WVC variability guides ASCAT and SCA users to infer, for example, 1-minute sustained winds from 20-km resolution [53,54] scatterometer measurements.

The connection of the SFMR wind reference at the extremes with absolute wind references from moored buoys between 15 and 25 m/s will be tested, as inconsistencies between them must be resolved. This leads to a recommended Cal/Val approach to assess the future C-band scatterometer high wind speed data during commissioning and operations. The methods and approach take into account the various uncertainty aspects, such as the representativeness of the data and the effects of collocation criteria.

5. Executive summary

The state of the art in ocean wind sensing is progressing and C-band radar well exploited. In addition, scatterometers, SAR, and microwave radiometers are exploited in other bands from Ku to L band. At the same time advisories on extreme winds are improving due to this expanded observation capability and due to associated improved modelling skills. However, both satellite measurements and models do need an absolute wind calibration reference in order to well describe the air-sea interaction processes and, above all, to provide accurate advisories. We note that, however, that the most adequate in situ references are more buoys and dropsondes provided by the NOAA hurricane hunters, but these wind references are inconsistent for wind speeds above 15 ms^{-1} .

The next steps for obtaining calibrated extreme satellite winds are described, exploiting a few decades of moored buoy data dropsondes. Since these references are generally not collocated, we compare both these in situ data sources with stable satellite, airplane and NWP references as a function of wind speed to investigate their respective relative biases. Since the NOAA hurricane hunter SFMR, ASCAT and ECMWF NWP model winds are a stable reference, the respective biases will determine the (in)consistency of moored buoy and dropsonde winds and, at the same time, provide a metric to obtain better absolute calibration of ASCAT, SFMR and ECMWF winds.

The SCA instrument will exploit a VH polarization channel, which has enhanced sensitivity at extreme winds. Using the results obtained above on absolute calibration, the VH GMF will be updated and extreme wind products will be defined for SCA during CHEFS.